Journal of Fluids and Structures 27 (2011) 1216–1227

Contents lists available at ScienceDirect

Journal of Fluids and Structures

journal homepage: www.elsevier.com/locate/jfs

On the aeroelastic transient behaviour of a streamlined bridge deck section in a wind tunnel

S. Manzoor [a], P. Hémon [a,*], X. Amandolese [b]

[a] LadHyX, CNRS-Ecole Polytechnique, F-91128 Palaiseau, France
[b] Chaire d'Aérodynamique, CNAM, Paris, France

ARTICLE INFO

Article history:
Received 10 September 2010
Accepted 12 July 2011
Available online 5 August 2011

Keywords:
Bridge deck
Flutter
Aeroelasticity
Wind tunnel
Transient
Temporal simulation

ABSTRACT

The study deals with the transient behaviour of a two degrees of freedom bridge deck section in a wind tunnel under the effect of an initial excitation. Response of the bridge deck section subjected to an initial mechanical excitation and excitation by an upstream gust is investigated separately. Experiments are conducted with three different frequency ratios between the plunge and pitch degrees of freedom. This experimental study shows that transient growth of energy occurs for wind velocities below the onset of flutter, reaching a level higher than 5 times the level of the initial excitation. In high wind conditions, this means that statistical or spectral computation techniques might underestimate the motion amplitude reached by a flexible bridge deck. This emphasises the importance of using temporal techniques under such circumstances.

1. Introduction

Temporal numerical simulations are increasingly performed in wind engineering studies because these calculations provide better estimations of structural constraints than the traditional spectral methods, even for a multimode study as in Jain et al. (1996). They also have the advantage of easily combining different kinds of load and can take nonlinearities into account.

In the case of wind-induced vibrations of flexible structures, such as bridge decks, the combination of wind turbulence excitation and aeroelastic effects can lead to new phenomena which are not always fully understood. Especially for high turbulent wind occurring close to the ground, the wind gusts act more as sudden transient excitations than as stationary excitation. In this context, a temporal simulation can be seen as a series of transient periods for which the response of the structure could be different than the response to statistically similar but stationary excitation. Temporal simulations have been studied before, for instance by Caracoglia and Jones (2003) and recently by Costa et al. (2007), but none of these approaches have considered the transient response of the structure. Therefore the careful study of transient phenomena is important.

In this paper the studied problem is restricted to a bridge deck section which is allowed to move in plunge and pitch. The transient aeroelastic response of this system is studied in a wind tunnel under an initial mechanical excitation and under a single gust superimposed to the mean velocity. The dynamical response of the system is studied in the stable regime of coupled-flutter instability, i.e. for mean velocities in the wind tunnel below the flutter critical velocity.

* Corresponding author. Tel.: +33 1 69 33 52 76; fax: +33 1 69 33 52 92.
E-mail address: pascal.hemon@ladhyx.polytechnique.fr (P. Hémon).

0889-9746/$ - see front matter
doi:10.1016/j.jfluidstructs.2011.07.003

Nomenclature

b B	span and chord of the bridge deck section (m)
$E(t)$	total energy versus time (J)
E_o	initial energy (J)
$E_{\max}$	maximum energy (J)
F_z	lift force (N)
f_α f_z	natural frequencies in torsion and in bending without flow (Hz)
f_1 f_2	frequencies of the coupled bending-torsion system (Hz)
J_O	inertia about O (kg m^2)
k_α k_z	stiffness in torsion and in bending (N m/rad and N/m, respectively)
m	mass (kg)
M_O	aerodynamic momentum about O (N m)
$\overline{U}$	mean wind velocity (m/s)
U_c	critical velocity of coupled mode flutter (m/s)
$\overline{U}/U_c$	velocity ratio
U_r	reduced velocity ($U_r=\overline{U}/B f_\alpha$)
$z(t)$	vertical displacement (m)
$\alpha(t)$	pitch angle (rad)
η_α η_z	reduced structural damping in torsion and in bending (%)

In previous work, similar experiments have already been conducted with a NACA airfoil (Hémon et al., 2006; Manzoor, 2010; Schwartz et al., 2009). These experiments have shown the existence of the so-called "transient growth of energy" mechanism which was theoretically studied by Schmid and de Langre (2003). This mechanism of transient growth can be described as an initial amplification of energy, followed by a monotonic decay due to the asymptotic stability of the system. Schmid and Henningson (2001) showed that it is a consequence of non-orthogonal modes involved in the system. It is strongly dependent on the initial conditions. In the case of the airfoil, transient growth of energy can lead to amplification by a factor up to 10 of the initial energy of the system and can even trigger the flutter instability in case of nonlinear structures (Schwartz et al., 2009).

However, the dynamics and the aeroelasticity of a bridge deck are quite different from those of an airfoil and justify the new experiments presented here. Most bridge deck sections, except very streamlined ones, behave like bluff bodies and the airflow is essentially separated downstream. Scanlan and Tomko (1971) showed conclusively that, though helpful, the Unsteady Airfoil Theory (Fung, 1993) has very distinct limitations in case of bridge deck sections. Aerodynamic flutter derivatives calculated even for streamlined bridge deck sections can show limited resemblance with those of a symmetric airfoil.

Moreover, the rotation centre of a deck is located in its middle by symmetry, while that of an airfoil is usually close to the first quarter of the chord. This leads to a pure structural coupling between the two degrees of freedom in case of the airfoil. For a bridge deck section on the other hand, coupling appears only by added aerodynamic terms.

In this paper we focus the study on the transient growth of energy mechanism, which is a new idea in the context of wind-induced vibrations of a bridge deck. Such a structure is classically not very sensitive to coupled mode flutter because of the design parameters. However, the transient behaviour, in relation to these design parameters, has not been investigated so far. The paper presents the experimental set-up and techniques and their validation. Transient results are presented first for a mechanical initial excitation. Then a wind gust is generated, identified and used to produce the initial excitation.

The aim of this paper is to present experimental evidence of the potentially high level of transient energy amplification, below critical flutter wind speed, due to extraneously excitation of a streamlined bridge deck section.

2. Experimental techniques

The experimental set-up is the one already used by Schwartz et al. (2009), except that it is adapted to the bridge deck instead of an airfoil. We recall here the main characteristics.

2.1. Experimental set-up

The bridge deck section has a hexagonal box shape typical of high aspect ratio streamlined deck with a chord, B=0.11 m, and a span, b=0.17 m. It is built from plexiglas using a numerical milling machine such that the surface is smooth and the edges almost sharp, Fig. 1. The experiment is conducted in an Eiffel wind tunnel, which has a closed square test-section of 0.180 m width. A 2500 W centrifugal fan downstream of the test-section produces the wind stream. The mean velocity in the test-section can vary from 4 to 25 m/s with a turbulence intensity level of 1.5% at 10 m/s.

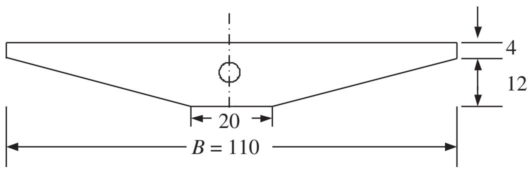

Fig. 1. Bridge deck cross-section schematic (dimensions in mm).

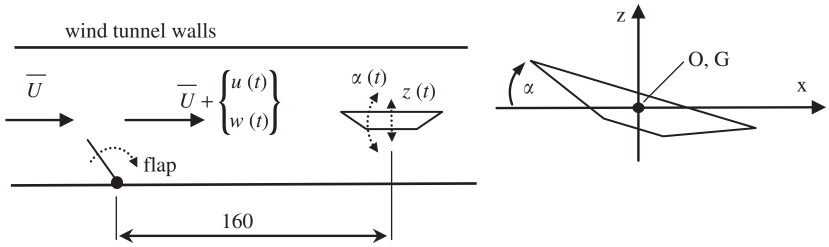

Fig. 2. Schematic of the bridge deck section in wind tunnel.

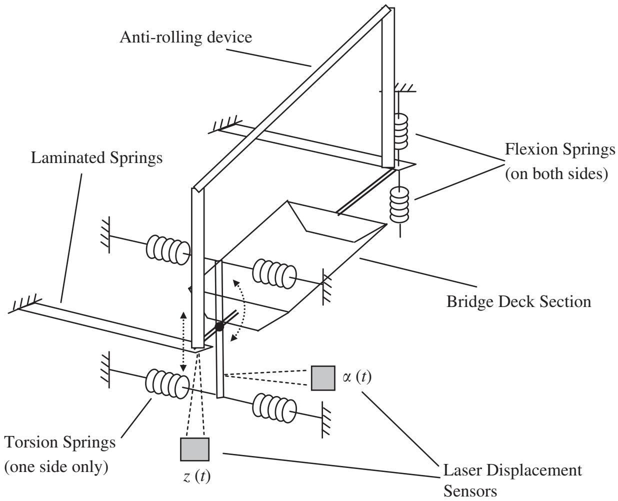

Fig. 3. Experimental set-up schematic.

The bridge deck section is supported at its axis of rotation which is located at its chord-wise geometric centre, Fig. 2. End plates are used at both the ends to impose a two-dimensional flow. Bearings support the suspended axis at the extremities of two long flat bands of aluminium alloy. Two sets of linear springs govern the torsional stiffness of the set-up. The flexural stiffness however, is controlled by a pair of vertically mounted linear springs on both sides of the model. The set-up is also rigged with an anti-rolling device, Fig. 3.

2.2. Measurement techniques

Motions of the model are obtained from two laser displacement sensors, one for the vertical linear motion and the other for the combined torsional and bending movement, Fig. 3. The measurement resolution is 40 μm and the accuracy is 1%. Signals from the laser displacement sensors are transmitted to an acquisition system PAK provided by Mueller-BBM; it consists mainly of a 24-bit and 8-channels acquisition card and signal processing software. The physical degrees of freedom $z(t)$ and $\alpha(t)$ are provided by the recombination of the measured signals using the system kinematics. Energy time history $E(t)$ is recovered directly within the measurement system by numerical post processing, as in Schwartz et al. (2009).

The reference mean wind velocity $\overline{U}$ is measured with a Pitot tube connected to an electronic manometer. A thermocouple measures the ambient temperature for correcting the reference wind velocity, with a precision of the order of 0.2%. Typical Reynolds number of the experiments, based on the chord, is in the range 35 000–160 000.

2.3. Identification of structural parameters

The equations of motion for the two degrees of freedom are provided for instance in Fung (1993):

$$m\ddot{z}+2m\eta_z\omega_z\dot{z}+k_z z=F_z,\quad J_O\ddot{\alpha}+2J_O\eta_\alpha\omega_\alpha\dot{\alpha}+k_\alpha\alpha=M_O. \tag{1}$$

Assuming that the structural damping is small, the eigenvalues can be written in the form:

$$\lambda_\alpha=\omega_\alpha^2=(2\pi f_\alpha)^2=k_\alpha/J_O;\quad \lambda_z=\omega_z^2=(2\pi f_z)^2=k_z/m. \tag{2}$$

Structural parameters are identified for each degree of freedom taken independently under zero wind velocity. Both the natural frequencies f_z and f_α are obtained by spectral analysis. A static weight calibration technique is used to calculate the stiffness k_z and k_α. The inertia J_O and mass m are then deduced, using

$$m = k_z/\lambda_z, \quad J_O = k_\alpha/\lambda_\alpha. \tag{3}$$

Pure structural damping values η_z and η_α are also determined using a standard decrement technique in free-decay tests.

The total energy is the sum of the system kinetic and potential energies:

$$E(t) = \tfrac{1}{2} m\dot{z}^2(t) + \tfrac{1}{2} J_O \dot{\alpha}^2(t) + \tfrac{1}{2} k_z z^2(t) + \tfrac{1}{2} k_\alpha \alpha^2(t). \tag{4}$$

Measurement of these structural parameters is reported in Table 1 for the three different cases studied, i.e. for the three different series of springs that were used to vary the frequency ratio between the two degrees of freedom.

For each case, the structural parameter measurement is validated by comparing an experimental free-decay test without wind, with results from numerical simulation of motion equations (1). Results are shown in Fig. 4 for Case 2. Initial conditions for each independent case are provided by small mechanically induced offsets. For the pure vertical displacement case, the laminated springs also introduce a small angle of rotation. This is taken into account in the recovery procedure of the laser signal. Close agreement of the experimental and simulation curves in Fig. 4 verifies the correct detection and measurement of various structural parameters of the bridge deck system.

The bridge deck section profile is not symmetrical; hence, as the wind flows around the deck section, a net mean lift force is generated which pushes the deck section downwards inducing a displacement from its rest position. This deflection remains constant with respect to time, but it is a function of the mean wind velocity $\overline{U}$. This deflection position is taken as the reference zero position for all the transient tests performed in the course of the present study. It means that, after an initial excitation, the bridge deck comes back to this position after its transient response, because all tests are performed with a mean velocity lower than the flutter critical velocity.

2.4. Aeroelastic parameters

Before studying the transient behaviour of our system, it is important to validate the system with standard measurements related to the long term stability. Firstly, the most important parameter is the flutter critical velocity because it will be used to reduce the wind velocity in the further transient study. For each case the critical velocity has been directly measured as the velocity when an unstable oscillation was reached. Results are plotted in Fig. 5 and listed in Table 2. Obviously the smallest critical velocity is obtained when the frequencies have the closest values. The second point is to observe the route to coupled mode flutter by measuring the frequencies evolution versus the mean velocity. The two frequencies f_1 and f_2 are normalised with the pure bending frequency and plotted as a function of the velocity ratio

Table 1
Structural parameters of different bridge deck sections studied.

	f_α/f_z	f_α (Hz)	f_z (Hz)	k_α (Nm/rad)	k_z (N/m)	J_O (kg m^2)	m (kg)	η_α (%)	η_z (%)
Case 1	1.185	8.00	6.75	1.85	1246.9	7.32e^{-4}	0.69	0.17	0.16
Case 2	1.606	7.12	4.43	1.33	519.4	6.64e^{-4}	0.66	0.3	0.08
Case 3	2.246	8.00	3.56	1.67	309.2	6.61e^{-4}	0.62	0.24	0.07

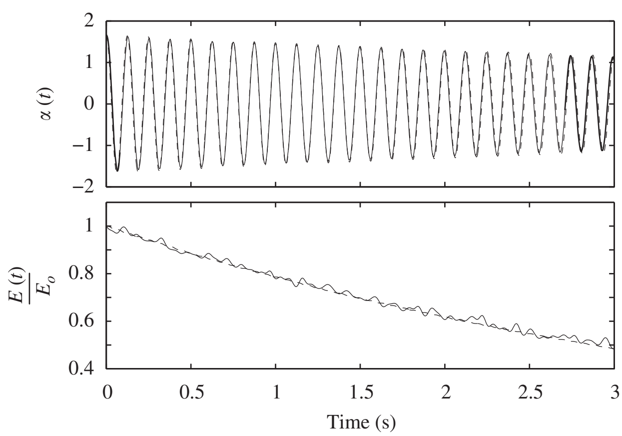

Fig. 4. Time evolution of angular displacement and corresponding dimensionless total energy for $\overline{U}=0$, $\alpha_o=1.66^\circ$, Case 2. —, experiment; - - -, computation.

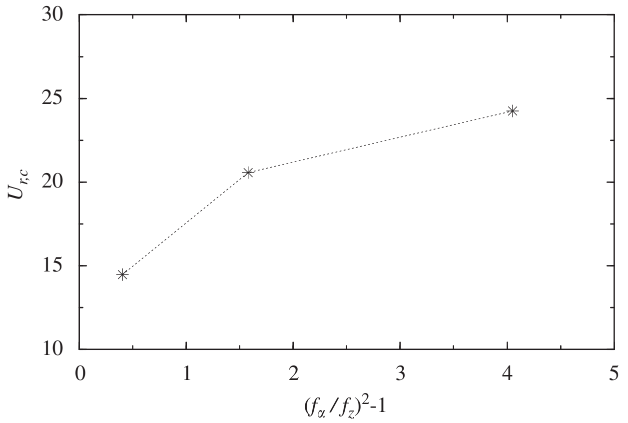

Fig. 5. Reduced critical velocity versus frequency ratio.

Table 2
Measured parameters of different bridge deck sections studied.

	f_α/f_z	U_c (m/s)	$U_{c,r}$	A_3	$(E_{\max}/E_o)_c$
Case 1	1.185	12.7	14.5	2.66	2.75
Case 2	1.606	16.1	20.6	2.53	5.0
Case 3	2.246	21.3	24.2	2.38	5.0

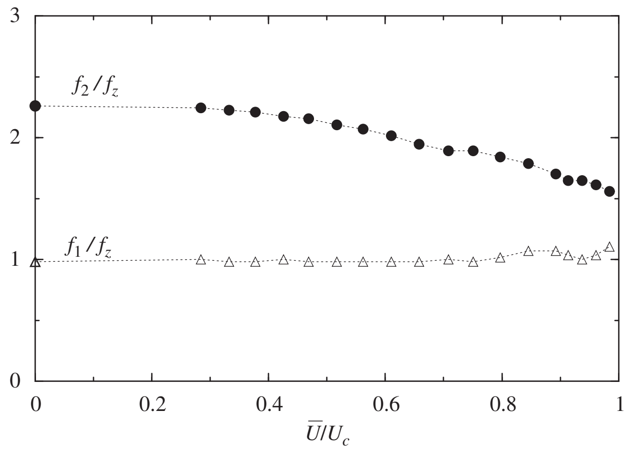

Fig. 6. Frequencies of the 2 modes versus velocity ratio, Case 3.

in Fig. 6. The lower branch in the plot is (f_1/f_z), where f_1 is the frequency of the vertical degree of freedom as it evolves with the wind velocity. Similarly, the upper branch in the plot is (f_2/f_z), where f_2 is the pitching frequency of the system. The behaviour agrees well with current knowledge on structurally uncoupled two degrees of freedom systems: the frequency of the heaving mode remains quasi-constant, while the frequency of the pitching mode decreases as the wind velocity increases, until they merge at the flutter critical velocity. Note that just before flutter, the pitching mode frequency decreases suddenly to reach at flutter a value slightly over the "pure" bending frequency.

Moreover, motion-induced aerodynamic terms could play an important role on the transient response of the system. According to Scanlan and Tomko (1971) the motion-induced aerodynamic loads can be approached using the following linear expressions introducing the so-called flutter derivatives. Retaining here only the terms that are important for the bridge deck flutter problem (Simiu and Scanlan, 1996), the equations of motion can be taken to be

$$m\ddot{z}+2m\omega_z(\eta_z+\eta a_z)\dot{z}+k_z z=0,\quad J_O\ddot{\alpha}+2J_O\eta_\alpha\omega_\alpha(\eta_\alpha+\eta a_\alpha)\dot{\alpha}+k_\alpha\alpha=\tfrac{1}{2}\rho U^2 bB^2 A_3\alpha. \tag{5}$$

In the present paper, only the uncoupled aerodynamic dampings ηa_α and ηa_z have been directly measured using free-decay tests in both pure pitching and plunging motion for various wind velocities. Results are given in Fig. 7. They are

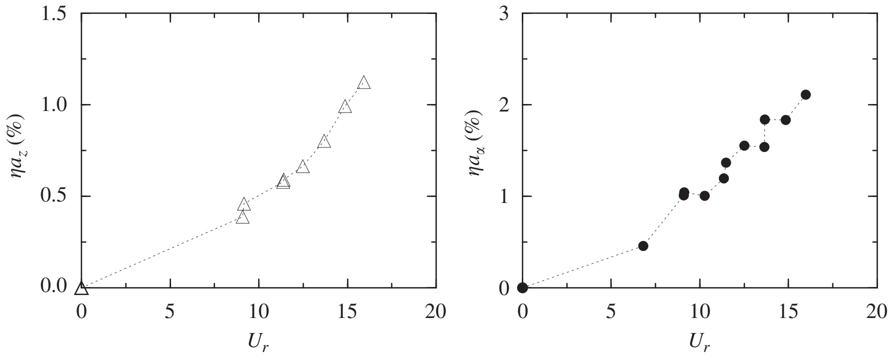

Fig. 7. Aerodynamic dampings versus reduced velocity, Case 1.

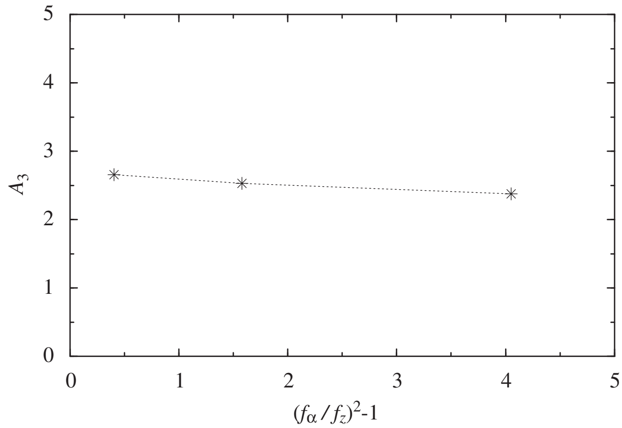

Fig. 8. Flutter derivative term A_3 deduced from critical velocity measurements versus frequency ratio.

expressed as reduced damping, so that they can be compared directly to the structural damping. According to the quasi-steady theory, the evolution of the aerodynamic damping is almost linear, which is approximately the case in our measurements. These results show also that there is no risk for single-degree-of-freedom flutter to occur, because the two damping values remain positive in the current range of wind velocity.

For the aerodynamic stiffness term A_3, an indirect procedure has been employed. Indeed, neglecting the structural and aerodynamic damping one can easily solve for the eigenvalues problem of the simplified system:

$$m\ddot{z}+k_z z=0, \quad J_O\ddot{\alpha}+k_\alpha\alpha=\tfrac{1}{2}\rho U^2 bB^2 A_3\alpha. \tag{6}$$

The onset of flutter for this system arises when the eigenvalues become complex, which corresponds physically to the velocity at which the torsional frequency catches up the bending frequency. Calculation leads to the following expression for the critical velocity (Hémon, 2006):

$$U_c=2\pi f_z\sqrt{\frac{2J_O}{\rho B^2 b}\frac{1}{A_3}\left(\left(\frac{f_\alpha}{f_z}\right)^2-1\right)}. \tag{7}$$

Using expression (7), aerodynamic stiffness A_3 can then be evaluated from the critical velocity measurements. Results reported in Fig. 8 confirm that, for highly reduced velocity, i.e. in the critical velocities range, the aerodynamic stiffness is quasi-constant and independent of the structural parameters used for the three cases tested.

3. Transient response to initial mechanical excitation

In this section, we study the transient response of the deck when subjected to an initial mechanical excitation. In the test procedure, an initial pitch angle α_0 is imposed on the deck, and then suddenly released. The data acquisition software permits automatic measurement and storage of experimental data for a pre-defined time interval. Energy of the bridge deck section, $E(t)$, is computed at the end of this recording period. The initial energy E_o, which serves as the reference energy, is deduced from the initial condition; in the present case it is the potential energy that is produced by the imposed initial pitch angle. One can also notice in Fig. 9 that the initial imposed pitch angle can be combined with a small initial deflection in z. Both α_o and z_o are used to calculate the initial energy E_o.

An example of the transient response of the bridge deck system due to the initial mechanical excitation can be observed in Fig. 9. The maximum energy ratio $E_{\max}/E_o$ is deduced from the time history $E(t)/E_o$. Tests are repeated a number of times for different mean wind velocities.

3.1. Effect of excitation amplitude

The effect of slight changes in the initial conditions on the maximum energy amplification is shown in Fig. 10. A dispersive effect can be observed as the velocity approaches the critical velocity of the system, i.e. as the velocity ratio approaches 1. Schmid and de Langre (2003) state that amplifying the initial perturbations may introduce nonlinear effects. In the present study, however, the magnitude of the initial mechanical excitations is varied within a very small range, i.e. $\sim 0.8^\circ$. The system is safely assumed to behave linearly for different initial conditions within this range.

Figs. 11 and 12 show sets of experimental data points obtained from a number of series to validate the reliability of the experimental technique under similar initial conditions between distinct experimental series.

3.2. Effect of frequency ratio

The energy evolution curves for all the three cases of frequency ratios exhibit similar behaviour, reaching a finite value before flutter. This maximum amplification value is shown in Fig. 13 as a function of the frequency ratio. It shows that,

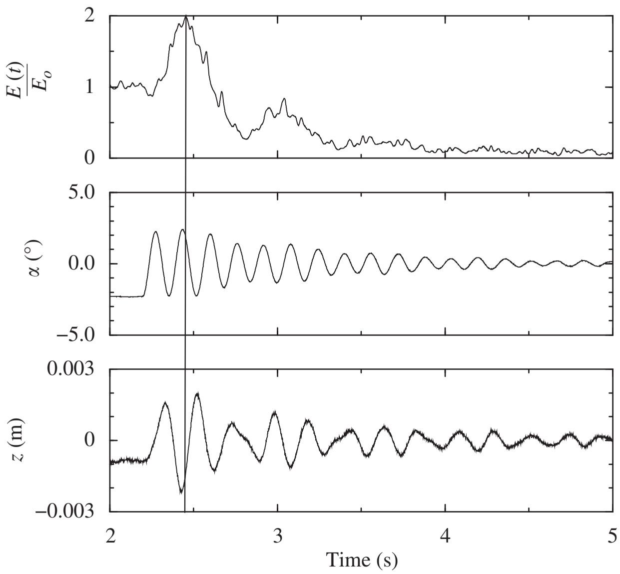

Fig. 9. Time evolution of energy, angular displacement and vertical displacement; mechanical excitation. $\overline{U}/U_c = 0.8$, Case 2 [$\alpha_o = -2.2^\circ$; $z_o = -0.92$ mm].

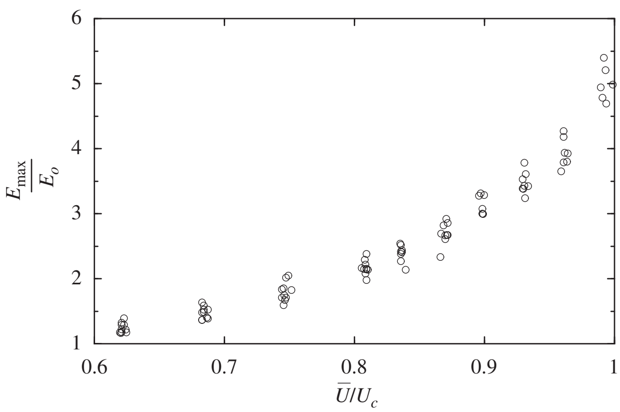

Fig. 10. Amplification rate of energy versus velocity ratio for Case 2; mechanical excitation with α_o varying from 1.8° to 2.6°.

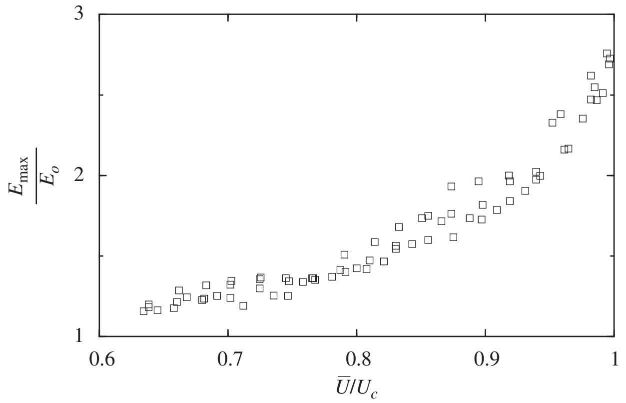

Fig. 11. Amplification rate of energy versus velocity ratio for Case 1; mechanical excitation.

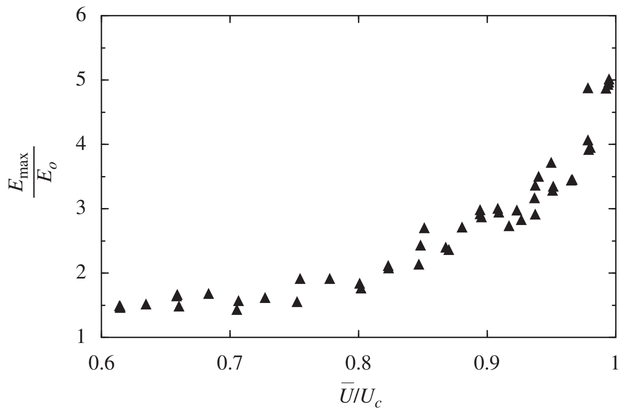

Fig. 12. Amplification rate of energy versus velocity ratio for Case 3; mechanical excitation.

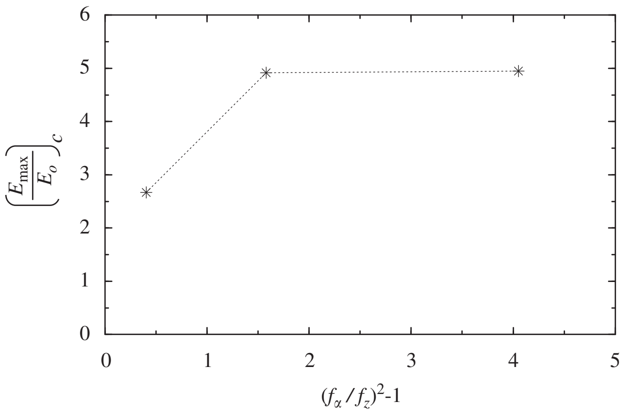

Fig. 13. Maximum energy amplification versus frequency ratio.

as the frequency ratio of the bridge deck section is increased, it seems that attainable energy amplification reaches a finite value close to 5. These data are also reported in Table 2.

However, this tendency cannot be disconnected from the dimensional value of the critical velocity of each case: the data presented in Fig. 13 are estimated at the critical conditions, just before flutter, which is indeed a function of the frequency ratio. Further investigation needs to be done in order to clarify this point.

4. Transient response to gust excitation

In the preceding section the bridge deck system was excited mechanically while the wind velocity remained constant throughout the interval of data accumulation. In this section, however, we present results obtained from a more realistic bridge deck experimental set-up involving an upstream gust. This gust impulse sets the system to oscillate upon interaction. Detailed description of the gust perturbation identification and the experimental set-up follows in the next sections.

4.1. Perturbation identification

An aluminium flap mounted on the test-section floor upstream of the bridge deck section is used to generate the perturbation, Fig. 2. The flap is 45 mm in length and 170 mm wide. The rotation axis of the flap is located 160 mm upstream of the deck section support point. Initially, the flap is held in position by a pre-tensioned spring. As the spring is released, the flap is set into motion creating a short impulse $u(t)$ and $w(t)$, which is added to the upstream velocity $\overline{U}$. Two-component hot wire anemometry is used to characterize the impulse. The horizontal component $u(t)$ of the impulse comprises a unique positive peak. The vertical component, however, has a negative peak followed by a positive peak. An example of the time evolution of both the orthogonal components is shown in Fig. 14. The time duration of the impulse is $\sim$0.02 s, which is well below the typical time period of the two degrees of freedom system.

An accelerometer is mounted on the flap to deduce the initial instantaneous reference. The signal from this accelerometer is also used to trigger data acquisition. This approach ensures that the data is accumulated from the same relative time instant in each repetition of the experiment. The impulse takes about 0.03 s to reach the leading edge of the deck section. This time interval is diminished as the wind velocity increases in the test-section.

Effects of any changes in the mean velocity $\overline{U}$ on the behaviour of the two component velocities are investigated in Fig. 15. These characteristic parameters of the upstream perturbation have been measured in the empty test-section at the position of the bridge deck section leading edge. For mean velocities greater than 12 m/s, the gust characteristics remain quasi-constant when they are reduced with the mean velocity. For this reason only bridge deck Cases 2 and 3 are studied in this section, their critical wind speed velocity being greater than 12 m/s.

4.2. Estimation of the initial energy

At the beginning of the test sequence, the bridge deck is allowed to respond freely to the incident flow. As the flap is released, a gust is created which excites the bridge deck. The bridge deck section then exhibits a transient response.

The time evolution of the angular and vertical displacements for a relative velocity $\overline{U}/U_c \approx 0.91$ is plotted in Fig. 16 for Case 3. The beginning of the transient response to the gust impulse corresponds well to the shape of the velocities generated by the flap: the deck motion starts with negative plunge and pitch, as the first event seen by the deck is a downward component of the velocity, see Fig. 14. Moreover, for this test, as for all the tests performed for Cases 2 and 3 at various wind speeds, the energy exhibits a distinct local peak in the time history occurring before the maximum energy peak due to the transient response. This local peak is clearly noticeable in Fig. 16 at a time close to 2.6 s. One can also notice that this local peak occurs when the deck reaches approximately the first minimum in plunge, while it reaches approximately the maximum velocity in pitch. All the energy calculations are then given relative to the mechanical energy E_o associated to this specific local peak, which can be viewed as the "gust energy" that is immediately transmitted to the deck before the transient growth amplification due to the dynamics of the system.

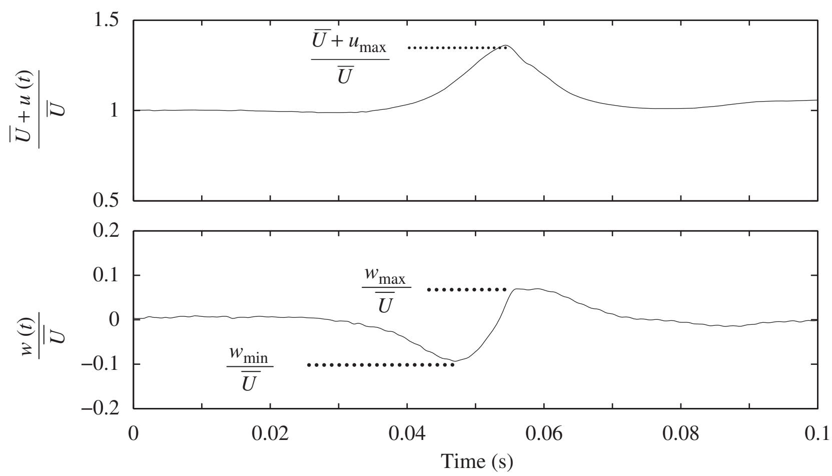

Fig. 14. Measured sample of upstream velocity perturbation.

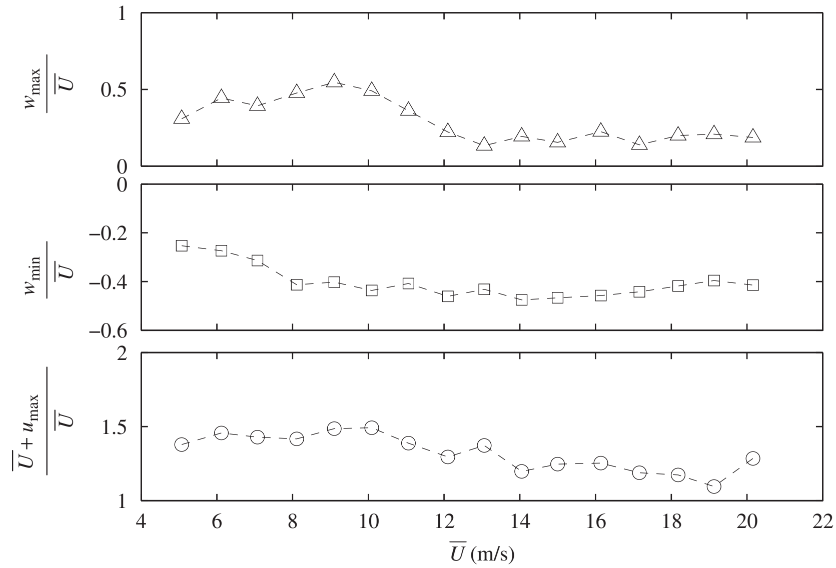

Fig. 15. Characteristics of the instantaneous upstream velocity perturbation versus mean velocity at the leading edge position.

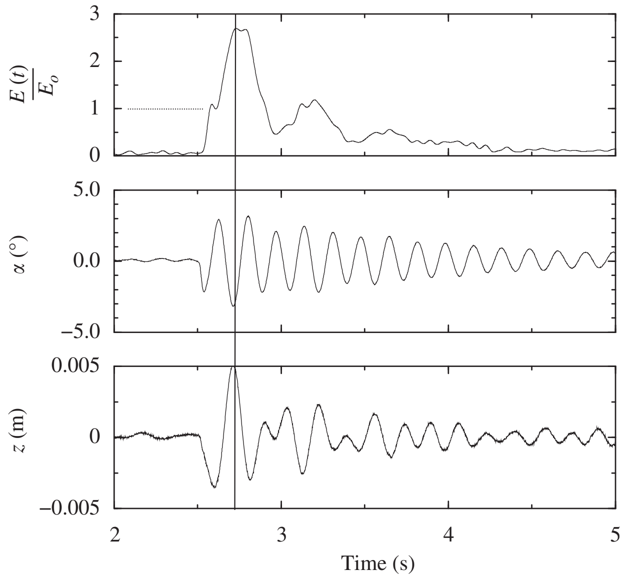

Fig. 16. Time evolution of energy, angular displacement and vertical displacement of the bridge deck section; excitation by flap. $\overline{U}/U_c = 0.95$, Case 3.

Values of this reference energy E_o are reported in Fig. 17 for both Cases 2 and 3 and various wind velocities. These results clearly show a covering domain (for velocity from 14 up to 16 m/s) for which E_o is close for the two Cases 2 and 3. This choice of E_o seems then to be independent of the dynamical system, but strongly linked to the energy of the gust impulse. This is also confirmed by the nearly quadratic evolution of E_o with the wind velocity in its higher range. Note that it is possible to extract a set of initial conditions (z_o, α_o, $\dot{z}_o$, $\dot{\alpha}_o$) from the time records, associated to the reference time t_0. By observing the curves, it is obvious that the two initial velocities $\dot{z}_o$ and $\dot{\alpha}_o$ are not zero, which is one of the main differences with the previous mechanical excitation.

4.3. Transient response

After the initial local peak the bridge deck exhibits a transient response which seems to be close to the one generated by a mechanical excitation. Nevertheless some discrepancies can be pointed out. When comparing for instance Figs. 9 and 16, it can be seen that the maximum energy level is obtained for different motion conditions: for mechanical excitation this

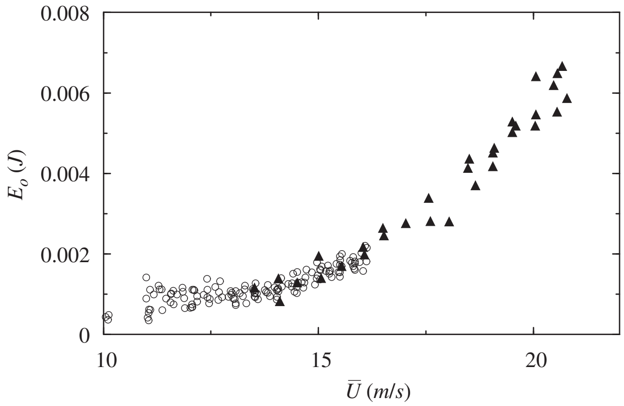

Fig. 17. Value of the reference energy E_o (J) versus mean velocity (m/s); ○, Case 2; ▲, Case 3; excitation by flap.

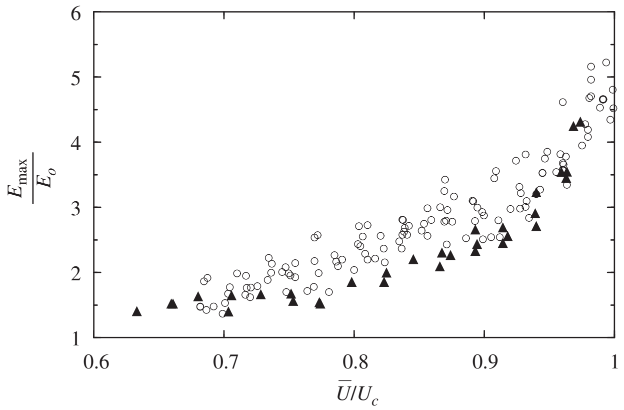

Fig. 18. Amplification rate of energy versus velocity ratio; ○, Case 2; ▲, Case 3; excitation by flap.

maximum occurs for a maximum pitch and minimum plunge, while for the gust excitation the maximum energy is obtained almost with a minimum pitch and a maximum plunge.

Fig. 18 shows the energy amplification behaviour of two deck section systems (Cases 2 and 3) subjected to an upstream gust. Gust monitoring for those experiments was carried out as described in previous section. The experimental data points show considerably lesser cohesion when compared to the previous experiments using fixed mechanical excitations.

Though the experimental points are easily distinguishable, they follow approximately the same trend as the velocity ratio increases. Indeed, just before flutter, the maximum energy ratio seems to be of the same order as the one observed with mechanical excitation.

5. Conclusion

An experimental set-up able to demonstrate the two degrees of freedom oscillations of a bridge deck section under the effect of an initial mechanical excitation and of an upstream gust, is developed. The set-up comprises a spring-mounted bridge deck section. An aluminium flap is used to create the upstream gust. Measurement techniques are tested and perfected to show reliable data acquisition during various experimental runs.

Experimental evidence is provided for the first time, linking the frequency ratio, the critical velocity and the maximum transient energy amplification of a bridge deck section in a wind tunnel. The transient growth of energy is found to have significant effects on the behaviour of the bridge deck. Energy amplification reaches up to 5 times the initial energy transmitted by the gust at a mean velocity just below the critical coupled mode flutter velocity.

As this configuration is reasonably a realistic scenario, the study shows that, in high wind conditions, the use of statistical techniques to compute the motion of a flexible bridge deck might miss the transient energy amplification and underestimate the motion amplitude reached by the deck. This study reinforces the interest of using temporal simulations for wind-induced vibrations of flexible structures.

In that context a transient formulation of the gust impulse based on the Küssner's function could be used for the buffeting terms along with a flutter-derivative formulation for the motion-dependent forces. Analysis of the time histories of the wind tunnel tests shows that the time scale of the gust is much lower than the characteristic period of the structural response, suggesting that there is no strong interaction between the gust and the aeroelastic response of the deck. However, even a streamlined bridge deck is really different from an airfoil for which the Theodorsen function is available. Therefore, the experimental study presented in this paper is necessary prior to the development of a theoretical model. Further works are ongoing in order to validate such a temporal model for transient growth study. Extensive parametric studies could then be done to highlight the impact of various parameters (frequency ratio, steady and unsteady aerodynamics coefficient of the bridge deck, gust time scales, etc.) to the potentially high level of transient energy amplification below critical flutter wind speed.

References

Caracoglia, L., Jones, N.P., 2003. Time domain vs. frequency domain characterization of aeroelastic forces for bridge deck sections. Journal of Wind Engineering and Industrial Aerodynamics 91, 371–402.

Costa, C., Borri, C., Flamand, O., Grillaud, G., 2007. Time domain simulations for wind-bridge interactions. Journal of Wind Engineering and Industrial Aerodynamics 95, 991–1006.

Fung, Y.C., 1993. An Introduction to the Theory of Aeroelasticity. Dover, New York.

Hémon, P., 2006. Vibrations des Structures Couplées Avec le Vent. Editions de l'Ecole Polytechnique, Palaiseau.

Hémon, P., de Langre, E., Schmid, P., 2006. Experimental evidence of transient growth of energy before airfoil flutter. Journal of Fluids and Structures 22, 391–400.

Jain, A., Jones, N.P., Scanlan, R.H., 1996. Coupled aeroelastic and aerodynamic response analysis of long-span bridges. Journal of Wind Engineering and Industrial Aerodynamics 60, 69–80.

Manzoor, S., 2010. Transient Instability Mechanisms by Frequency Coalescence in Fluid-Structure Systems. Ph.D. Thesis, Ecole Polytechnique, Palaiseau, France.

Scanlan, R.H., Tomko, J.J., 1971. Airfoil and bridge deck flutter derivatives. ASCE Journal of the Engineering Mechanics Division 1717–1737

Schmid, P., de Langre, E., 2003. Transient growth before coupled-mode flutter. Journal of Applied Mechanics 70, 894–901.

Schmid, P., Henningson, D.S., 2001. Stability and Transition in Shear Flows. Springer, New York.

Schwartz, M., Manzoor, S., Hémon, P., de Langre, E., 2009. By-pass transition to airfoil flutter by transient growth due to gust impulse. Journal of Fluids and Structures 25, 1272–1281.

Simiu, E., Scanlan, R.H., 1996. Wind Effects on Structures. Wiley and Sons, New York, pp. 461–464.